Biochimica et Biophysica Acta 1828 (2013) 708–714

Contents lists available at SciVerse ScienceDirect

Biochimica et Biophysica Acta

journal homepage: www.elsevier.com/locate/bbamem

Lipid-like behavior of signal sequence peptides at air–water interface

Ernesto E. Ambroggio, Gerardo D. Fidelio *

Centro de Investigaciones en Química Biológica de Córdoba, (CIQUIBIC, UNC–CONICET), Departamento de Química Biológica, Facultad de Ciencias Químicas, Universidad Nacional de Córdoba, Haya de la Torre y Medina Allende, Ciudad Universitaria, X5000HUA, Córdoba, Argentina

ARTICLE INFO

Article history:
Received 9 May 2012
Received in revised form 18 October 2012
Accepted 5 November 2012
Available online 13 November 2012

Keywords:
Signal sequence peptide
Peptide monolayer
Peptide–lipid interaction
PM-IRRAS
Lateral surface stability
Interfacial peptide structure

ABSTRACT

Several protein transport processes in the cell are mediated by signal sequence peptides located at the N-terminal side of the mature protein sequence. To date, the specific interaction and the stability of these peptides at the amphipathic interface of biological membranes and the relevance of the peptide conformation when they interact with lipids is not clear. We report the surface properties and the peptide–lipid interaction of three signal sequence peptides at the air–NaCl 145 mM interface by using the Langmuir monolayer approach. These synthetic peptides have a natural sequence with a non-periodic amphiphilicity, where hydrophobic and hydrophilic residues are located on opposed sides of the peptide primary sequence. We show that signal sequence peptides form insoluble monolayers of high stability against lateral compression. At close packing, peptide molecular area, surface potential and the high stability of the peptide monolayer are indicative that signal sequence peptides are compatible with a β-sheet conformation at the interface. Structure was confirmed with PM-IRRAS and transmission FT-IR studies. The peptides show lateral miscibility with either POPC (a liquid-expanded lipid) or DPPC (a liquid-condensed lipid) in mixed peptide–lipid monolayers. This indicates that signal sequence peptides studied are laterally miscible with phospholipids independent of the phase state of the lipid.

© 2012 Elsevier B.V. All rights reserved.

1. Introduction

Signal sequence peptides (SSP) are N-terminal extensions of newly synthesized proteins that need to face membranes, for example the ER, mitochondria, the thylakoid compartment, etc. [1,2]. Signal sequence peptides have a wealth of functional information, they have high homology, all have a hydrophobic core (H-region) rich in Phe, Leu, Ileu, Met, Val, Trp, a positively charged amino terminal region (N-region) and a polar carboxy-terminal C-region [3]. They contain specific information for performing distinct functions for protein targeting and membrane insertion and also play an important role after their cleavage from the parent protein [4–6].

The recent review of Matlin [7] celebrating the 40th anniversary of the launch of the signal hypothesis, firstly presented by Blobel and Sabattini in 1971 [8], gives a summary for the huge amount of work done on this topic and emphasizing all the protein machinery involved in protein translocation. SSP can direct proteins thorough different translocation pathways. Proteins can be co- or post-translational targeted to membranes when still unfolded. The Sec translocon machinery assists the transport of non-mature proteins in a SRP dependent or independent way. Recently, the structure of SSP bound to *Methanococcus jannaschii* SRP core was reported at 3 Å resolution [9]. The Tat-system is another SSP mediated system but independent of the Sec apparatus identified in chloroplast and bacteria, where its distinctive feature is a twin arginine localized immediately up stream in the H-region of the SSP [10].

Recently it was suggested, for transmembranes helices insertion, that a minimum of leucine residues in a synthetic construct are needed to overcome the energetic cost of hydrophobic mismatch and it is improved if lysine residues are flanking the peptide segment. The authors concluded that the recognition of the transmembrane segment by the translocon machinery involves *physical partitioning* of the non-periodic amphiphilic peptide into phospholipids [11]. The intimate contact of SSP with lipids once targeted to the membrane has been corroborated by crosslinking experiments [6]. During or after translocation, SSPs are cleaved off by a signal peptidase [6,12]. Furthermore, it was claimed that SSPs within the membrane can be additionally processed by intramembrane presenilin-like proteases (SSP–peptidase) promoting fragments with potential biological effects after membrane desorption or removal [13]. So, in the one-way dynamic path of the SSP from the insertion to its removal, there would be no doubt that in the time in which SSP is intimately interacting with membrane lipids, the interaction should be compatible with the non-leaky properties of the membrane. The ability to keep the permeability barrier of the membrane during protein translocation take places, in both co- and post-translational translocation and in all the subsequent steps, has been recently considered by Rapoport [6]. Although, the role of membrane lipids has been rather unconsidered and, far less the surface properties of signal sequences.

Abbreviations: SSP, signal sequence peptide; ASS, human albumin signal sequence peptide; ESS, signal sequence peptide of rat elastase; PM-IRRAS, polarized-modulated infrared reflection-absorption spectroscopy; PSS, dog pretrypsinogen signal sequence peptide; RTP, chloroplast transit peptide of the Ribulose 1,5-bis-phosphate carboxylase-oxygenase

* Corresponding author. Tel.: +54 351 4334168 int 3465.
E-mail address: gfidelio@dqb.fcq.unc.edu.ar (G.D. Fidelio).

0005-2736/$ – see front matter © 2012 Elsevier B.V. All rights reserved.
http://dx.doi.org/10.1016/j.bbamem.2012.11.004

However, several authors have claimed a more active role of lipids in protein translocation with emphasis in the thermodynamic viability and energetic requirements of the process [14–18].

Within these functions, we are interested on the physical bases of how SSPs interact with the membrane lipids before its cleavage [10]. For this direct membrane–peptide interaction, the individual interfacial physical properties of the SSPs and their interaction with lipids have to be determinant. In order to better understand the physics involved in this SSP–lipid association, we have studied the individual surface properties of three different SSP and their interaction with lipids that present different phase state at the interface (POPC, a fluid lipid and DPPC, a condensed lipid), at the air–NaCl 145 mM interface. Also, we compared the interfacial properties of the SSPs with the previously reported data of other membrane-interacting peptides like melittin [19], the antibiotic peptides Maculatin and Citropin [20], the chloroplast transit peptide of the Ribulose 1,5-bis-phosphate carboxylase-oxygenase (RTP) [21] and the transmembrane M1 segment from the acetylcholine receptor [22]. The approach used for all surface studies, analyzing pure peptides and peptide–lipid mixtures, was the Langmuir monolayer technique. Also, we have determined the secondary structure of the peptides either in bulk (in presence of SDS micelles) or directly at the air–NaCl interface where the SSPs are organized as a pure peptide monolayers. We used transmission Fourier-transformed infrared (FT-IR) spectroscopy for the bulk measurements and polarized-modulated infrared reflection-absorption spectroscopy (PM-IRRAS) in order to assess peptide structure at the air–NaCl interface.

From monolayers composed of SSPs, we found that the human albumin signal sequence peptide (ASS), the dog pretrypsinogen signal sequence peptide (PSS), and the signal sequence peptide of the rat elastase (ESS) (Table 1) have a remarkable high stability against lateral compression. From peptide–lipid mixed monolayers all three peptides were miscible with POPC and DPPC where ASS and PSS form ideal mixtures while ESS–lipid mixed monolayers show repulsive forces. Structural analyses gave us the evidence that the peptides preferentially adopt a β-sheet structure either in bulk or at the air–NaCl interface, and this structure may confer the high stability to the peptide in a amphiphilic environment.

2. Materials and methods

2.1. Lipids and reagents

2 Dipalmitoyl-sn-Glycero-3-Phosphocholine and 1-palmitoyl-2-Oleoyl-sn-Glycero-3-Phosphocholine lipids (DPPC and POPC respectively) were purchased from Avanti Polar Lipids co (Alabaster, AL, USA), ^2H_2O and SDS from Sigma-Aldrich Chem. Co. (St. Louis. MO, USA).

2.2. Peptides source

Peptides were synthesized on p-alkoxybenzylpolystyrene with flourenylmethoxycarbonyl protected amino acids on an Milligen 9050 Peptide Synthesiser using the protocol described by the manufacturers, cleaved and de-protected by incubation in 50% TFA, 5% anisole, 2.5% ethyl methyl sulphide and 42.5% dichloromethane for 2 h, triturated in diethyl ether, then purified by reverse-phase HPLC on a C8 Rainin column as previously reported [21,23]. ASS was synthesized during a stay of GDF in the laboratory of Dr. Brian Austen, Department of Surgery, St. George's Hospital Medical School, London. Samples of PSS and ESS were kindly donated by Dr. Austen.

Table 1
Peptide primary structure.

Human Albumin Signal Sequence (ASS)
LYS-TRP-VAL-THR-PHE-ILE-SER-LEU-LEU-PHE-LEU-PHE-SER-SER-ALA-TYR-SER
Trypsinogen Signal Sequence (PSS)
ALA-LYS-LEU-PHE-LEU-PHE-LEU-ALA-LEU-LEU-LEU-ALA-TYR-VAL-ALA
Rat Elastase Signal Sequence (ESS)
LEU-ARG-PHE-LEU-VAL-PHE-ALA-SER-LEU-VAL-LEU-TYR-GLY-HIS-SER-THR-GLU-ASP-PHE-PRO-GLU-THR-ASN-ALA

2.3. FT-IR experiments

Transmission FT-IR spectra of signal sequence peptides (6.7 mg/ml) in a 15% SDS solution in ^2H_2O were recorded 12 h after sample preparation (to ensure a complete H/D exchange) on a Nicolet Nexus spectrometer (Thermo Scientific, West Palm Beach, FL), at room temperature in a CaF_2 cell with a 0.1 μm Teflon spacer. Before FT-IR measurements, the peptides were lyophilized several times from 10 mM HCl in order to eliminate traces of TFA. The IR chamber was continuously purged with dry air to eliminate water vapour interference. 100 scans were signal-averaged at a resolution of 2 cm^{-1} and the spectra of peptide-free samples were subtracted from the spectra of the peptide-containing samples by using OMNIC E.S.P. 5.1 (Thermo Scientific, West Palm Beach, FL) software. Fourier self-deconvolution was performed and the values for the bandwidth and the enhancement for the deconvoluted spectra were 18 cm^{-1} and 2, respectively. The band fitting was performed as described by Nolan et al. [24].

2.4. PM-IRRAS experiments

PM-IRRAS was performed using a KSV PMI 550 instrument (KSV Instruments Ltd. Helsinki, Finland) with a built in Fourier Transform IR-spectrometer in similar way as described by Vico et al. [25]. One arm of the goniometer bears a PM-unit (ZnSe photoelastic modulator) and a highly sensitive MCT-detector is mounted on the other arm. The spectra were acquired with a resolution of 8 cm^{-1} over a spectral range of 800–4200 cm^{-1}. The Langmuir trough (32.7 cm x 7.5 cm; volume = 150 mL) was set up so that the light beam reached the monolayer at a fixed angle of incidence of 80°and the frequency of wavelength modulation used was 1500 cm^{-1}. The incident light was continuously modulated between s and p polarization at a high frequency (2f = 100 kHz). This allows the simultaneous measurement providing the reference spectrum. Because the spectra are measured simultaneously the effect of water is largely reduced. The baseline was acquired on a peptide-free NaCl 145 mM solution (subphase). Each spectrum was obtained with 6000 scans accumulation at a temperature of 23–25 °C. Pure peptide monolayers were formed by direct spreading from a chloroform: methanol (2:1, v/v) solution by using a micro-syringe and the solvent was allowed to evaporate for at least 5 min before compression was started.

2.5. Langmuir monolayer experiments

Langmuir monolayer experiments of pure peptide or peptide–lipid mixture were also performed using a home-made equipment where the total surface area of the Teflon trough was 80 cm^2 and the volume of the subphase was 75 ml as previously reported [20]. As for PM-IRRAS experiments, lipids and peptides were dissolved in chloroform: methanol (67:33, v/v) solution. For peptide–lipid mixed monolayers, peptides and lipids were premixed at the desired proportion from their respective pure solutions, and then directly spread onto the surface. The surface pressure (Π) (measured employing the Wilhelmy method via platinized-Pt plate), the area enclosing the monolayer, and the surface potential (ΔV) (determined with a milliVoltmeter detecting the tension generated between an air-ionizing ^{241}Am plate and a calomel electrode pair) were automatically measured (with the control unit Monofilmmeter with Film Lift, Mayer Feintechnique, Göttingen, Germany). The data were recorded continuously and simultaneously with a double channel X-YY recorder.

3. Results

3.1. Pure peptide monolayers

Fig. 1A shows the surface lateral pressure and surface potential (Π and ΔV) versus molecular area (A) compression isotherms of pure signal sequence peptide monolayers at the air–NaCl interface. Like other signal sequence peptides [23], these peptides have a high lateral collapse pressure (Π_c) of about 40 mN/m. The collapse pressure is an useful parameter to measure the lateral stability [26,27]. The higher is Π_c much more stable is the monolayer against lateral compression. To be comparative, the collapse pressure observed for the signal sequence peptides is quite close to the Π_c observed for pure lipid monolayers, molecules that conform very stable monolayers. Also, Π_c is the point of the highest lateral molecular packing of the molecules restricted at the monomolecular array. At this point it is possible to assess the molecular area occupied for each peptide and to measure the dipolar contributions of the confined molecules to the surface potential. We found that ASS and PSS have a molecular area of 0.50 and 0.60 nm^2/molecule, respectively, accompanied by rather low values of surface potential. For ESS a higher molecular area and surface potential was observed, more compatible with a β-hairpin perpendicular to the surface. The surface parameters for the three signal sequence peptides are summarized in Table 2. From geometrical analyses, the most probable secondary structure that can be inferred for the peptides from these data (low molecular area and surface potential) is a β-sheet structure perpendicular to the interface (see Fig. 1B). In order to corroborate this deduced structure we performed Fourier-transformed infrared spectroscopy (FT-IR) and polarized-modulated infrared reflection-absorption spectroscopy (PM-IRRAS). Both techniques allow for directly determining the protein secondary structure of the peptides either in bulk solution (FT-IR) or directly at the air–NaCl interface (PM-IRRAS).

3.2. FT-IR spectroscopy of signal sequence peptides in the presence of SDS micelles

The FT-IR technique it is a well-known technique that allows to straightforwardly measure the secondary structure of peptides and proteins. The amide I absorption band (between 1700 and 1600 cm^{-1}) is associated mainly to the stretching of the C O and C—N groups of the peptide bond where each secondary structure shows a characteristic absorption band [24,28].

From Fig. 2A, B and C, it is possible to see that the main absorption bands in the amide I region for the signal sequence peptides in presence of the SDS micelles (15% in ^2H_2O) are located around 1622 and 1626 cm^{-1}. These frequencies are characteristic of the β-sheet secondary structure [28]. In Fig. 2A, B and C we also summarizes band contributions to the amide I region for ASS, ESS and PSS. We have chosen SDS micelles to mimic amphiphilic environment in bulk since it was used for many authors in the past to explore the structure of cleavable

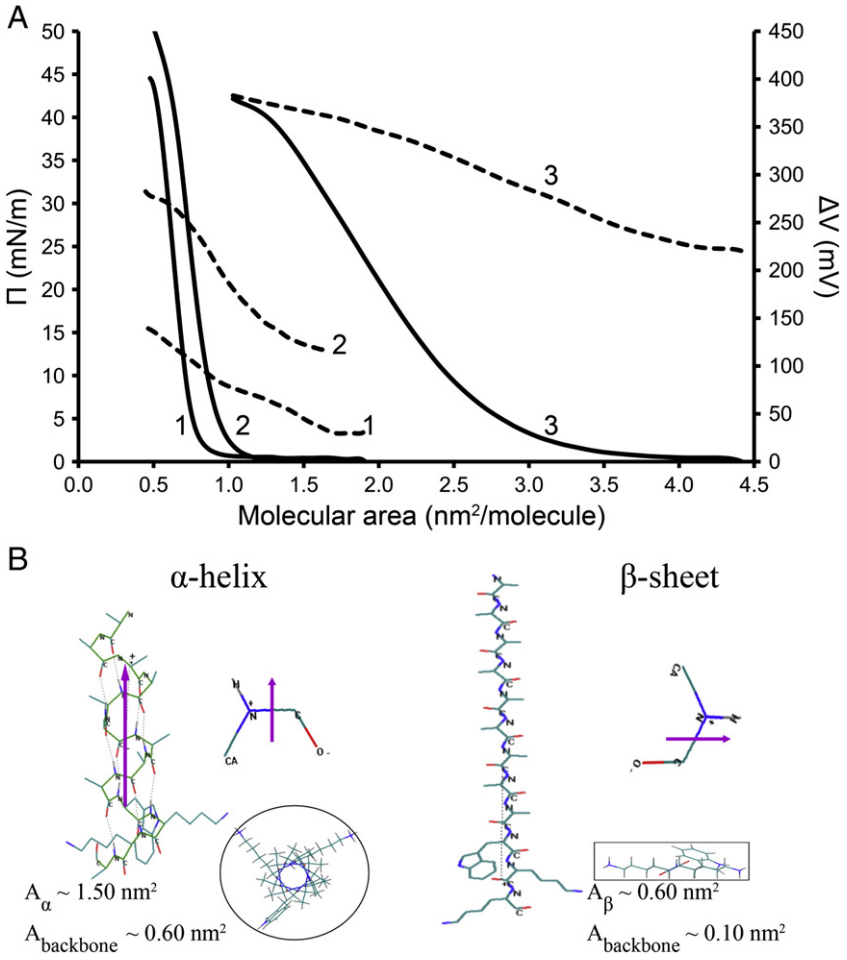

Fig. 1. Pure peptide monolayers. (A) ΠA (solid line) and ΔVA (dashed line) compression isotherms of pure ASS (1), PSS (2) and ESS (3) monolayers. Subphase: NaCl 145 mM (pH 6). (B) Molecular model of a α-helix (left) and a β-sheet (right) peptide perpendicular to the interface. Note the difference in areas for the transversal cut of each structure (circle and rectangle, respectively). Purple arrow denotes the dipole contribution of the peptide bond for each structure. It is remarkable how an α-helical peptide perpendicular shows a macro-dipole as a result of the sum of the single dipoles from of each peptide bond. The contrary is seen for a β-sheet peptide perpendicular to the interface where the dipole of the peptide bond cancels each other in this array.

Table 2
Surface and molecular parameters of pure signal sequence peptide monolayers.

Peptide	Molecular area (nm^2/molecule)	Collapse pressure (mN/m)	Surface potential (mV)
ASS	0.5	38	130
PSS	0.6	42	250
ESS	1.4	41	380

and non-cleavable SSPs [29–36]. SDS was also used to study the structure adopted by the transmembrane M1 segment from the acetylcholine receptor [22], the well known amphiphilic melittin [37] which surface properties and lipid miscibility at air–water interface was available [19,22]. All these previous reported evidences allow us the comparison of the data in similar systems.

3.3. PM-IRRAS of signal sequence peptides at the air–NaCl interface

From the FT-IR data it is clear that the peptides in bulk adopt mainly a β-sheet structure. We wanted to know whether this was the same when the peptides were conforming monolayers at the air–NaCl interface. To measure this, we took advantage of the PM-IRRAS technique. As for transmission FT-IR, in PM-IRRAS the most useful information about protein secondary structure comes from the Amide I band [38,39]. Fig. 2D shows the PM-IRRAS spectra of ASS, PSS and ESS at high molecular packing. As can be observed, a strong band is present around 1620 cm^{-1} for ESS and ASS while PSS presents two typical signals at 1633 cm^{-1} and 1660 cm^{-1} all corresponding to a β-sheet peptide array at the interface [38,40]. For comparison purposes we also included the measurements from a monolayer composed by the lytic α-helical peptide melittin. As it can be appreciated the difference is clear-cut. Melittin does not have the characteristic β-sheet bands found in spectra of the signal sequence peptides and, on the other hand, shows a strong band around 1650 cm^{-1}, characteristic of a α-helix.

3.4. Mixed peptide–lipid monolayers

From the above-described data, we now wanted to know how β-sheet peptides interact with lipids in mixed peptide–lipid monolayers when lipids have different physical properties at the air–NaCl interface. In order to answer this, we investigated the behavior of mixed SSP/lipid monolayers using POPC, an expanded lipid, and DPPC, a condensed lipid when lateral pressure is higher than 15 mN/m. Mixed with either POPC or DPPC we found that all three signal sequence peptides are miscible with the lipids. This is concluded since a single collapse pressure (Π_c) is observed from the Π–A compression isotherms of the mixed monolayers (Fig. 3, see surface phase rule in [26]). This behavior was always observed regardless the peptide–lipid ratio. Moreover, as expected for a miscible behavior, the Π_c of mixed peptide–lipid monolayer depends on the proportion of the components in the mixture (see [26]).

Also, we wanted to understand whether the mixed peptide–lipid monolayers behaved as ideal or non-ideal mixtures. For this purpose we compared the ideal area that the mixed monolayer would have with the experimental area (obtained from the compression isotherms of the peptide–lipid monolayers) using the following equation (Eq. (1)):

$$(A_{\text{ideal}})_P = \left(A_{\text{lipid}}\right)_P X_{\text{lipid}} + \left(A_{\text{peptide}}\right)_P X_{\text{peptide}} \quad (1)$$

where A_{lipid} and A_{peptide}, are the respective individual molecular areas taken from the pure lipid or peptide compression isotherms at a specific surface pressure Π. X_{lipid} and X_{peptide} are the mole fraction of each component in the mixed monolayer. From these analyses we found that for ASS and PSS, either mixed with POPC or DPPC, there were no significant deviations from the ideal regime (Fig. 4). On the other hand, ESS showed a positive deviation (Fig. 4) when mixed with DPPC or POPC. This means that repulsive forces would be playing an important role for this mixture [27]. In addition, for all signal sequence peptides mixed with DPPC, it is possible to see that the liquid expanded to liquid condensed phase

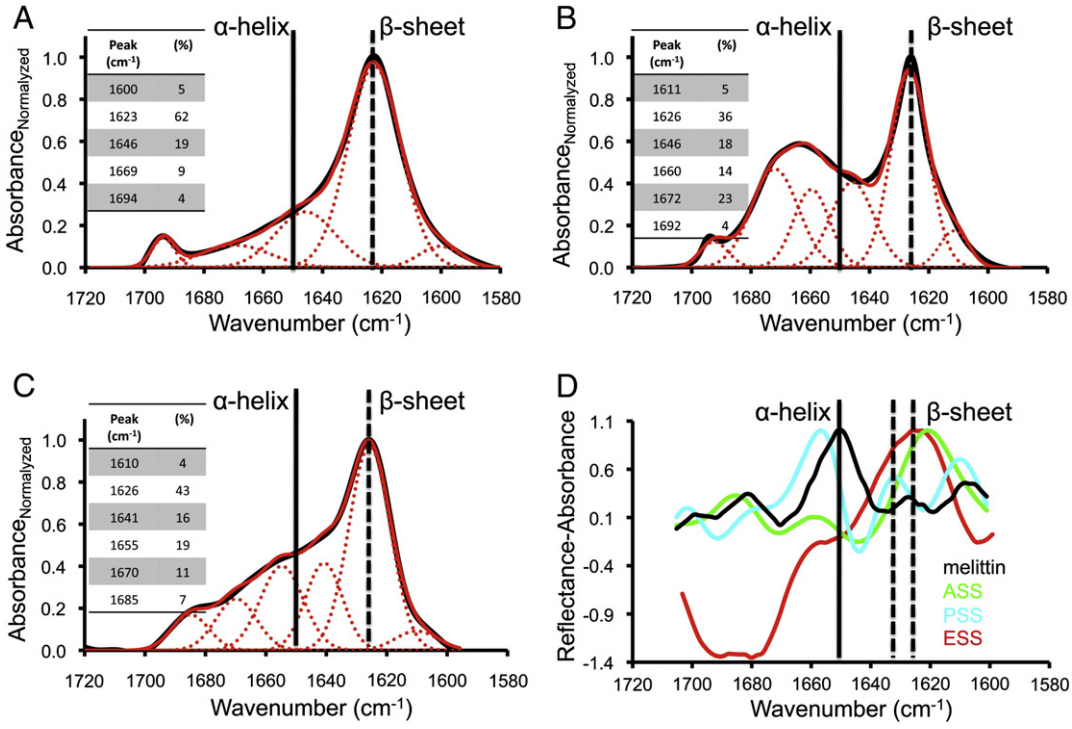

Fig. 2. Structural analyses of signal sequence peptides. Transmission FT-IR of ASS (A), PSS (B) and ESS (C) suspended in 15% SDS (^2H_2O). The black spectrum corresponds to the experimental FT-IR signal while the red spectrum is the calculated spectrum that results from the fitted Gaussian bands (red dashed curves). (D) PM-IRRAS spectra obtained from melittin (black), ASS (green), PSS (cyan) and ESS (red) monolayers at maximal packing (16, 35, 23 and 35 mN/m, respectively). Subphase: NaCl 145 mM (pH 6). The vertical lines indicate the typical frequencies for an α-helix (solid) or a β-sheet (dashed) conformation.

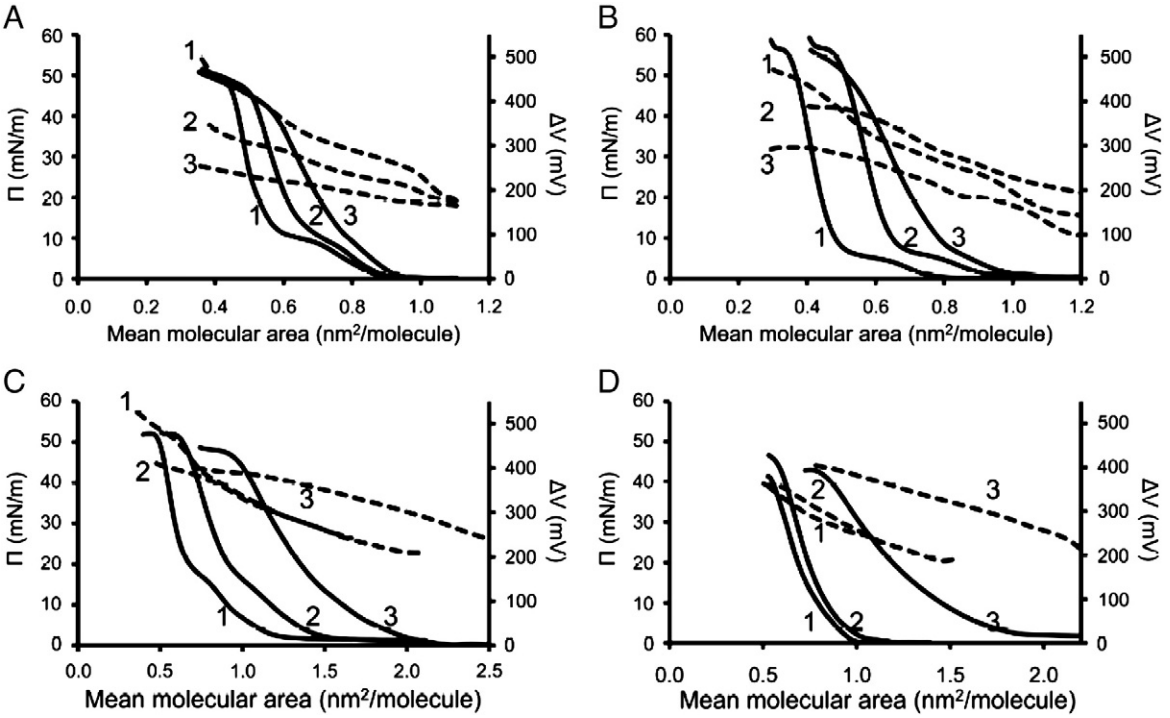

Fig. 3. Signal sequence peptide–lipid mixed monolayers. Π-A (solid line) and ΔV-A (dashed line) compression isotherms of DPPC-ASS (A), DPPC-PSS (B) and DPPC-ESS (C) at peptide–lipid area proportions of 0.25–75 (1), 0.5–0.5 (2) and 0.75–0.25 (3). (D) Π-A (solid line) and ΔV-A (dashed line) compression isotherms of POPC-ASS (1), POPC-PSS (1) and POPC-ESS (3) at the peptide–lipid area proportion of 1:1. Subphase: NaCl 145 mM (pH 6).

transition is less noticeable as the peptide mole ratio increases (Fig. 3A, B and C).

4. Discussion

In agreement with previous findings [23], our results show that monolayers of SSPs have high stability against the lateral compression at the air–NaCl interface. We attributed this stability as the effect of having a peptide monolayer where the molecules adopt a β-sheet secondary structure and then presenting the possibility to form an infinite planar array on the interface with a high degree of molecular self-association [23,41–43]. We confirmed this secondary structure by directly measuring the peptide secondary structure either in bulk or in-situ on the air–NaCl interface. In addition, the low surface potential showed by these peptides can be attributed to this structure too because the dipole of the peptide bond might be parallel to the plane of the interface (Fig. 1B), contrasting with the higher surface potential found for both more helical amphipathic peptides, checked in similar systems, such as melittin [19] or the transmembrane M1 segment from the acetylcholine receptor [22]. ASS and PSS have a clear β-sheet profile with a compatible molecular area of an extended β-strand perpendicular to the interface. The peptide corresponding to EES sequence shows an important shoulder at 1670 cm^{-1} in its FT-IR profile (Fig. 2) compatible with a β-hairpin structure, in keeping with the higher molecular area certainly found for this peptide.

From mixed peptide–lipid monolayers we found an interesting behavior. DPPC and POPC were used in this work because they have a marked difference in the interfacial physical properties (DPPC has a liquid expanded to liquid condensed phase transition in contrast with POPC that is a full liquid-expanded lipid). With both lipids all the peptides have lateral miscibility at the all peptide–lipid mole ratio studied. PSS and ASS showed an ideal behavior when the experimental area of the mixture is compared with the ideal area. A different observation was found for ESS where positive deviations from the ideal mixture

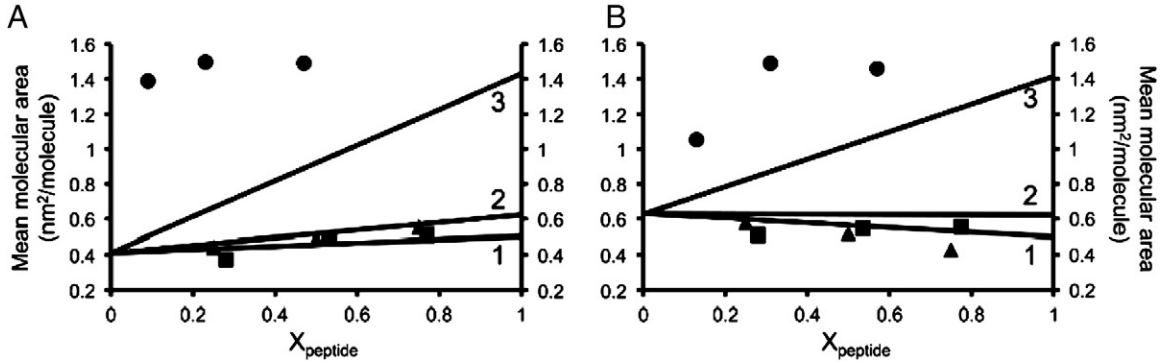

Fig. 4. Interaction within components in a peptide–lipid mixed monolayer. Ideal mean molecular area (solid line) compared with the experimental mean molecular area (see Eq. (1)), obtained from the compression isotherms of the signal sequence peptide–lipid monolayers (symbol) at different peptide–lipid ratios. (A) DPPC and (B) POPC mixed with ASS, (line 1, square), PSS (line 2, triangle) and ESS (line 3, circle). Subphase: NaCl 145 mM (pH 6).

were observed (Fig. 4). This reflects that there are repulsive interactions between the components of the mixed monolayer. This can be due to the presence of charged residues in the peptide sequence (see Table 1) and also that part of the sequence of the mature protein is present in the peptide sequence (Table 1). Additionally, it is interesting to denote that in mixed SSP–DPPC monolayers the liquid expanded → liquid condensed phase transition was still observable at low peptide–lipid ratios but barely noticed when the peptide proportion was high. Probably this points out that the presence of SSPs can fluidize the lipid phase, a fact that would be very interesting to measure by using fluorescence microscopy coupled to the Langmuir monolayer technique.

From our laboratory, several reports describing the surface properties of monolayers composed by α-helical peptides have been published. We find several differences in the surface properties and in the peptide–lipid interaction of the signal sequence peptides in comparison to those of the α-helical peptides (melittin [19], the antibiotic peptides Maculatin and Citropin [20], the chloroplast transit peptide of ribulose 1, 5 bisphosphate carboxilase-oxygenase [21] and the transmembrane M1 segment from the acetylcholine receptor [22]). These α-helical peptides form insoluble monolayers with low Π_c, meaning that this structure has a low degree of self-association and then generating monolayers with low stability, a remarkable difference with the high stability of the monolayers made of SSPs. Also, α-helical peptides show a completely immiscible behavior with phosphocholine lipids reflecting that miscibility can be a typical property of peptides that adopt a β-structure at the interface, like the studied SSPs. Another important difference is that the surface potential of α-helical peptides is clearly higher than the surface potential of the signal sequence peptides. In our model (Fig. 1B), the reason of this difference might be because there is a dipole summation from the peptide bond in the α-helix structure perpendicular to the interface, generating a macro-dipole. On the other hand, the dipole of a β-sheet peptide oriented perpendicular to the interface would lay parallel to this plane avoiding a macro-dipole formation [44–46].

The secondary structure of SSPs in amphipathic medium is still a matter of debate [16,17,29–31,33,35,47–51]. Some authors reported that a β-sheet structure was compatible with functionality [29,47]. Batemburg et al. [30] found a α-helical in SDS micelles but a predominant β-sheet structure in Lubrol detergent or in lysoPC micelles for PhoE signal sequence. Briggs et al. [48] and Cornell et al. [51] testing the λ receptor and LamB protein from *E. coli*, respectively, found either α-helix or β-sheet depending on the lateral surface pressure in which the films were the films were transferred to solid substrates before ATR-FTIR and CD analyses. From all these data, SSPs may be considered as adaptable molecules to fit and face the different translocation steps confined to a restricted space at the amphiphilic membrane. The recent report of Hainzl et al. [9] by which a structural flexibility was observed on the hydrophobic pocket of SSP–SRP interaction domain does not invalidate with our data.

5. Conclusions

How is the protein transport and translocation thorough the membrane? How is the protein–lipid interaction at the interface as a product of this transport? These questions are the reason of several studies developed from several decades to this date. Our experimental results led us to conclude that the analyzed SSPs interact with model membranes, are incorporated into the lipid monolayer, and resist high lateral pressures at the interface. This study also shows that the kind of interaction may depend on the secondary structure that the peptide adopts at the interface. SSPs, which present a β-sheet structure at the interface, show a miscible behavior independently of the physical state of the lipid. This can be biologically relevant for the transport of proteins because it involves a complex machinery, and the transport could be possible because the peptides do not have a preferential interaction with lipids in a determinate physical-state and resist high lateral forces that allow the SSP to remain inserted in the membrane. Taken together all this property appears as relevant in order to keep the amphipathic membrane sealed during translocation and further SSP processing.

Acknowledgments

We wish to thank Dr. Brian Austen for providing the peptides. Financial support was provided by research funds from SeCyT (Universidad Nacional de Córdoba), CONICET and ANPCyT (Argentina). E.E.A is a recently reentry fellow (Beca de reinserción) from CONICET and G.D.F is a member of the Scientific Research Career (CIC) from CONICET (Argentina).

References

[1] L.M. Gierasch, Signal sequences, Biochemistry 28 (1989) 923–930.
[2] P. Walter, A.E. Johnson, Signal sequence recognition and protein targeting to the endoplasmic reticulum membrane, Annu. Rev. Cell Biol. 10 (1994) 87–119.
[3] G. von Heijne, Transcending the impenetrable: how proteins come to terms with membranes, Biochim. Biophys. Acta 947 (1988) 307–333.
[4] N. Zheng, L.M. Gierasch, Signal sequences: the same yet different, Cell 86 (1996) 849–852.
[5] R.S. Hegde, V.R. Lingappa, Membrane protein biogenesis: regulated complexity at the endoplasmic reticulum, Cell 91 (1997) 575–582.
[6] T.A. Rapoport, Protein translocation across the eukaryotic endoplasmic reticulum and bacterial plasma membranes, Nature 450 (2007) 663–669.
[7] K.S. Matlin, Spatial expression of the genome: the signal hypothesis at forty, Nat. Rev. Mol. Cell Biol. 12 (2011) 333–340.
[8] G. Blobel, D.D. Sabatini, Ribosome–Membrane Interaction in Eukaryotic Cells, in: L.A. Manson (Ed.), Biomembranes, vol. 2, Plenum Publishing Corporation, New York, 1971, pp. 193–195.
[9] T. Hainzl, S. Huang, G. Merilainen, K. Brannstrom, A.E. Sauer-Eriksson, Structural basis of signal-sequence recognition by the signal recognition particle, Nat. Struct. Mol. Biol. 18 (2011) 389–391.
[10] B. Martoglio, B. Dobberstein, Signal sequences: more than just greasy peptides, Trends Cell Biol. 8 (1998) 410–415.
[11] S. Jaud, M. Fernandez-Vidal, I. Nilsson, N.M. Meindl-Beinker, N.C. Hubner, D.J. Tobias, G. von Heijne, S.H. White, Insertion of short transmembrane helices by the Sec61 translocon, Proc. Natl. Acad. Sci. U. S. A. 106 (2009) 11588–11593.
[12] A. Weihofen, K. Binns, M.K. Lemberg, K. Ashman, B. Martoglio, Identification of signal peptide peptidase, a presenilin-type aspartic protease, Science 296 (2002) 2215–2218.
[13] B. Martoglio, Intramembrane proteolysis and post-targeting functions of signal peptides, Biochem. Soc. Trans. 31 (2003) 1243–1247.
[14] S.H. White, Translocons, thermodynamics, and the folding of membrane proteins, FEBS Lett. 555 (2003) 116–121.
[15] M. Bogdanov, W. Dowhan, Lipid-assisted protein folding, J. Biol. Chem. 274 (1999) 36827–36830.
[16] R.C. Keller, J.A. Killian, B. de Kruijff, Anionic phospholipids are essential for alpha-helix formation of the signal peptide of prePhoE upon interaction with phospholipid vesicles, Biochemistry 31 (1992) 1672–1677.
[17] T. Ahn, D.B. Oh, H. Kim, C. Park, The phase property of membrane phospholipids is affected by the functionality of signal peptides from the *Escherichia coli* ribose-binding protein, J. Biol. Chem. 277 (2002) 26157–26162.
[18] T.J. McIntosh, A. Vidal, S.A. Simon, The energetics of binding of a signal peptide to lipid bilayers: the role of bilayer properties, Biochem. Soc. Trans. 29 (2001) 594–598.
[19] G.D. Fidelio, B. Maggio, F.A. Cumar, Interaction of melittin with glycosphingolipids and phospholipids in mixed monolayers at different temperatures. Effect of the lipid physical state, Biochim. Biophys. Acta 862 (1986) 49–56.
[20] E.E. Ambroggio, F. Separovic, J. Bowie, G.D. Fidelio, Surface behaviour and peptide–lipid interactions of the antibiotic peptides, Maculatin and Citropin, Biochim. Biophys. Acta 1664 (2004) 31–37.
[21] E.E. Ambroggio, B. Austen, G.D. Fidelio, Biophysical properties of a synthetic transit peptide from wheat chloroplast ribulose 1,5-bisphosphate carboxylase, J. Pept. Sci. 13 (2007) 245–252.
[22] E.E. Ambroggio, M.A. Villarreal, G.G. Montich, D.T. Rijkers, M.R. De Planque, F. Separovic, G.D. Fidelio, Interfacial properties of the M1 segment of the nicotinic acetylcholine receptor, Biophys. Chem. 121 (2006) 171–176.
[23] G.D. Fidelio, B.M. Austen, D. Chapman, J.A. Lucy, Properties of signal-sequence peptides at an air–water interface, Biochem. J. 238 (1986) 301–304.
[24] V. Nolan, M. Perduca, H.L. Monaco, B. Maggio, G.G. Montich, Interactions of chicken liver basic fatty acid-binding protein with lipid membranes, Biochim. Biophys. Acta 1611 (2003) 98–106.
[25] R.V. Vico, R.H. de Rossi, B. Maggio, PM-IRRAS assessment of the compression-mediated orientation of the nanocavity of a monoacylated beta-cyclodextrin in monolayers at the air-water interface, Langmuir 26 (2010) 8407–8413.
[26] G.L. Gaines, Insoluble Monolayers at Liquid–Gas Interfaces, Interscience, New York, 1966.
[27] K.S. Birdy, Lipid and Biopolymers Monolayers at Liquid Interfaces, Plenum Press, New York, 1989.

[28] J.L. Arrondo, A. Muga, J. Castresana, F.M. Goni, Quantitative studies of the structure of proteins in solution by Fourier-transform infrared spectroscopy, Prog. Biophys. Mol. Biol. 59 (1993) 23–56.
[29] G.L. Reddy, R. Nagara, Circular dichroism studies on synthetic signal peptides indicate beta-conformation as a common structural feature in highly hydrophobic environment, J. Biol. Chem. 264 (1989) 16591–16597.
[30] A.M. Batenburg, R. Brasseur, J.M. Ruysschaert, G.J. van Scharrenburg, A.J. Slotboom, R.A. Demel, B. de Kruijff, Characterization of the interfacial behavior and structure of the signal sequence of *Escherichia coli* outer membrane pore protein PhoE, J. Biol. Chem. 263 (1988) 4202–4207.
[31] B. Bechinger, Structure and dynamics of the M13 coat signal sequence in membranes by multidimensional high-resolution and solid-state NMR spectroscopy, Proteins 27 (1997) 481–492.
[32] V. Chupin, J.A. Killian, J. Breg, H.H. de Jongh, R. Boelens, R. Kaptein, B. de Kruijff, PhoE signal peptide inserts into micelles as a dynamic helix-break-helix structure, which is modulated by the environment. A two-dimensional 1H NMR study, Biochemistry 34 (1995) 11617–11624.
[33] Y. Yamamoto, T. Ohkubo, A. Kohara, T. Tanaka, M. Kikuchi, Conformational requirement of signal sequences functioning in yeast: circular dichroism and 1H nuclear magnetic resonance studies of synthetic peptides, Biochemistry 29 (1990) 8998–9006.
[34] S.H. Portlock, Y. Lee, J.M. Tomich, L.K. Tamm, Insertion and folding of the amino-terminal amphiphilic signal sequences of the mannitol and glucitol permeases of Escherichia coli, J. Biol. Chem. 267 (1992) 11017–11022.
[35] L.A. Correll, T.A. Woodford, J.D. Corbin, P.L. Mellon, G.S. McKnight, Functional characterization of cAMP-binding mutations in type I protein kinase, J. Biol. Chem. 264 (1989) 16672–16678.
[36] C.J. McKnight, M.S. Briggs, L.M. Gierasch, Functional and nonfunctional LamB signal sequences can be distinguished by their biophysical properties, J. Biol. Chem. 264 (1989) 17293–17297.
[37] H. Raghuraman, A. Chattopadhyay, Effect of micellar charge on the conformation and dynamics of melittin, Eur. Biophys. J. 33 (2004) 611–622.
[38] Z. Xu, J.W. Brauner, C.R. Flach, R. Mendelsohn, Orientation of peptides in aqueous monolayer films. Infrared reflection-absorption spectroscopy studies of a synthetic amphipathic beta-sheet, Langmuir 20 (2004) 3730–3733.
[39] R. Mendelsohn, J.W. Brauner, A. Gericke, External Infrared Reflection Absorption Spectrometry of Monolayer Films at the Air-Water Interface, Annu. Rev. Phys. Chem. 46 (1995) 305–334.
[40] G. Thakur, M. Micic, R.M. Leblanc, Surface chemistry of Alzheimer's disease: a Langmuir monolayer approach, Colloids Surf. B Biointerfaces 74 (2009) 436–456.
[41] E.E. Ambroggio, D.H. Kim, F. Separovic, C.J. Barrow, K.J. Barnham, L.A. Bagatolli, G.D. Fidelio, Surface behavior and lipid interaction of Alzheimer beta-amyloid peptide 1–42: a membrane-disrupting peptide, Biophys. J. 88 (2005) 2706–2713.
[42] R. Maget-Dana, The monolayer technique: a potent tool for studying the interfacial properties of antimicrobial and membrane-lytic peptides and their interactions with lipid membranes, Biochim. Biophys. Acta 1462 (1999) 109–140.
[43] R. Maget-Dana, D. Lelievre, A. Brack, Surface active properties of amphiphilic sequential isopeptides: Comparison between alpha-helical and beta-sheet conformations, Biopolymers 49 (1999) 415–423.
[44] A. Wada, The alpha-helix as an electric macro-dipole, Adv. Biophys. (1976) 1–63.
[45] W.G. Hol, The role of the alpha-helix dipole in protein function and structure, Prog. Biophys. Mol. Biol. 45 (1985) 149–195.
[46] W.G. Hol, Effects of the alpha-helix dipole upon the functioning and structure of proteins and peptides, Adv. Biophys. 19 (1985) 133–165.
[47] M.P. Caulfield, K. Park, M. Rosenblatt, G.D. Fasman, Correlation of secondary structure with biological activity for a leader peptide: circular dichroism-derived structure and in vitro biological activities of preproparathyroid hormone peptide and its analogs, Arch. Biochem. Biophys. 289 (1991) 208–213.
[48] M.S. Briggs, D.G. Cornell, R.A. Dluhy, L.M. Gierasch, Conformations of signal peptides induced by lipids suggest initial steps in protein export, Science 233 (1986) 206–208.
[49] S.W. Chi, G.S. Yi, J.Y. Suh, B.S. Choi, H. Kim, Structures of revertant signal sequences of Escherichia coli ribose binding protein, Biophys. J. 69 (1995) 2703–2709.
[50] L. Voglino, T.J. McIntosh, S.A. Simon, Modulation of the binding of signal peptides to lipid bilayers by dipoles near the hydrocarbon-water interface, Biochemistry 37 (1998) 12241–12252.
[51] D.G. Cornell, R.A. Dluhy, M.S. Briggs, C.J. McKnight, L.M. Gierasch, Conformations and orientations of a signal peptide interacting with phospholipid monolayers, Biochemistry 28 (1989) 2789–2797.